

Understanding the geodetic signature of large aquifer systems: Example of the Ozark Plateaus in Central United States

Stacy Laroche¹, Kristel Chanard^{2,3}, Luce Fleitout⁴, Jérôme Fortin⁵, Adriano Gualandi⁶, Laurent Longuevergne⁷, Paul Rebischung^{2,3}, Sophie Violette^{4,8}, and Jean-Philippe Avouac¹

¹ Geological and Planetary Sciences, California Institute of Technology, Pasadena, California, USA

² Université de Paris, Institut de physique du globe de Paris, CNRS, IGN, Paris, France

³ ENSG-Géomatique, IGN, Marne-la-Vallée, France

⁴ Laboratoire de Géologie, École Normale Supérieure, Université PSL, CNRS, Paris, France

⁵ University PSL, CNRS UMR 8538, Paris, France

⁶ Istituto Nazionale di Geofisica e Vulcanologia, Bologna, Italy

⁷ Univ Rennes, CNRS, Geosciences Rennes - UMR 6118, F-35000 Rennes, France

⁸ Sorbonne University, UFR.918, Paris, France

Contents of this file

Figures S1 to S9

Table S1

Introduction

The following files contains 9 figures and 1 table supporting the findings of the manuscript.

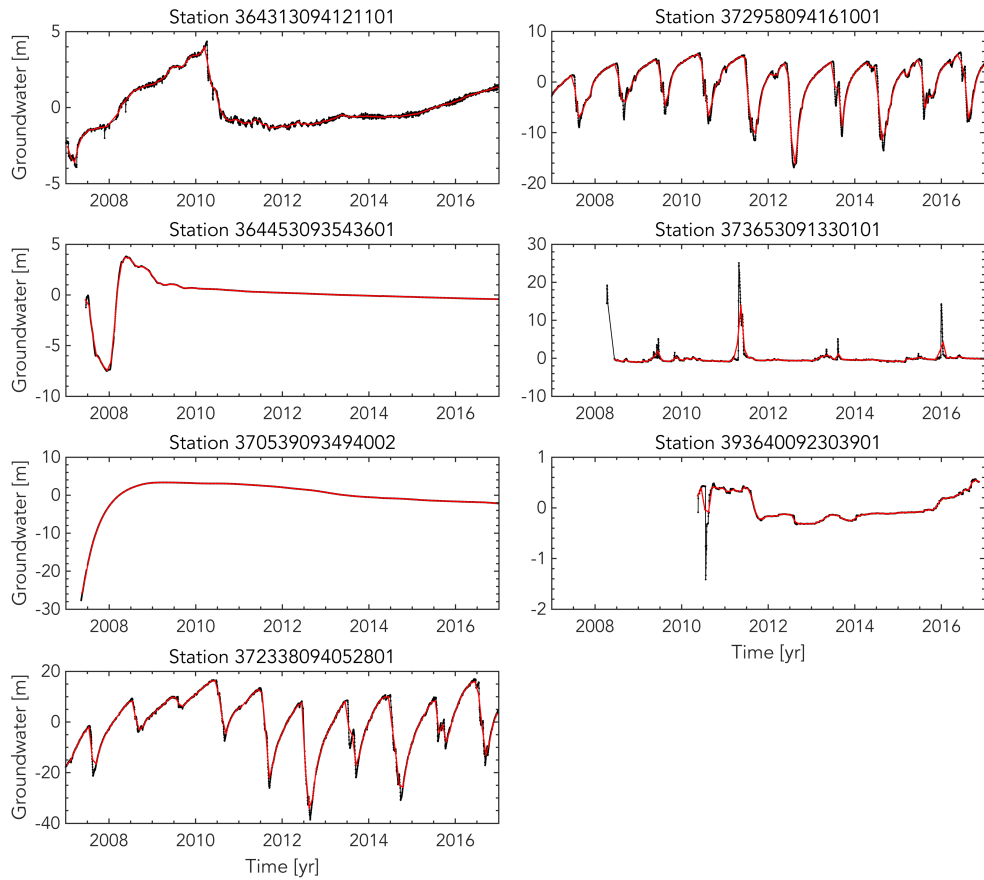
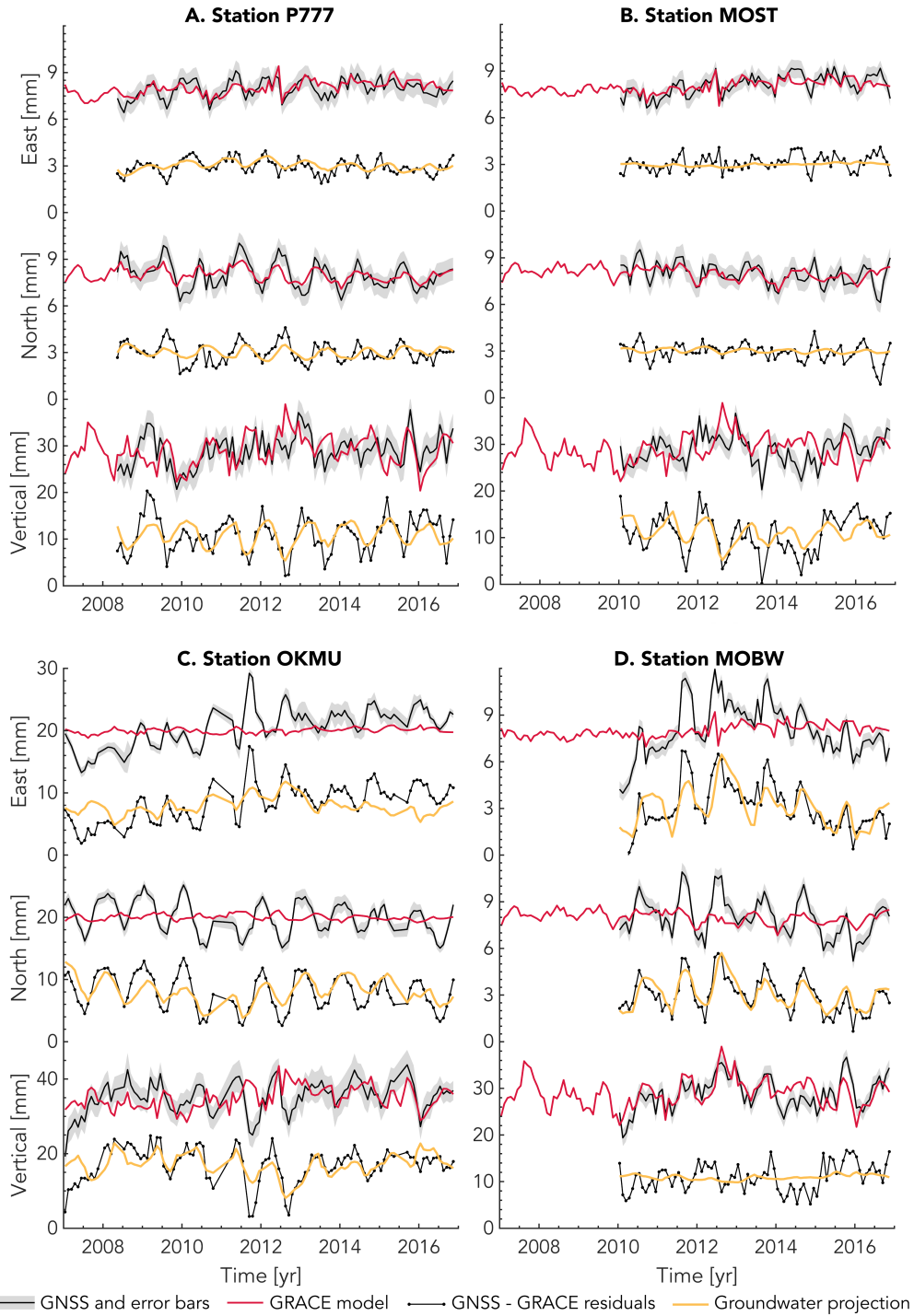


Figure S1: Groundwater time series excluded from the analysis. Black dots are the raw daily data and the red lines are the monthly averages. Stations 372958094161001 and 372338095042801 likely reflect local pumping effects.



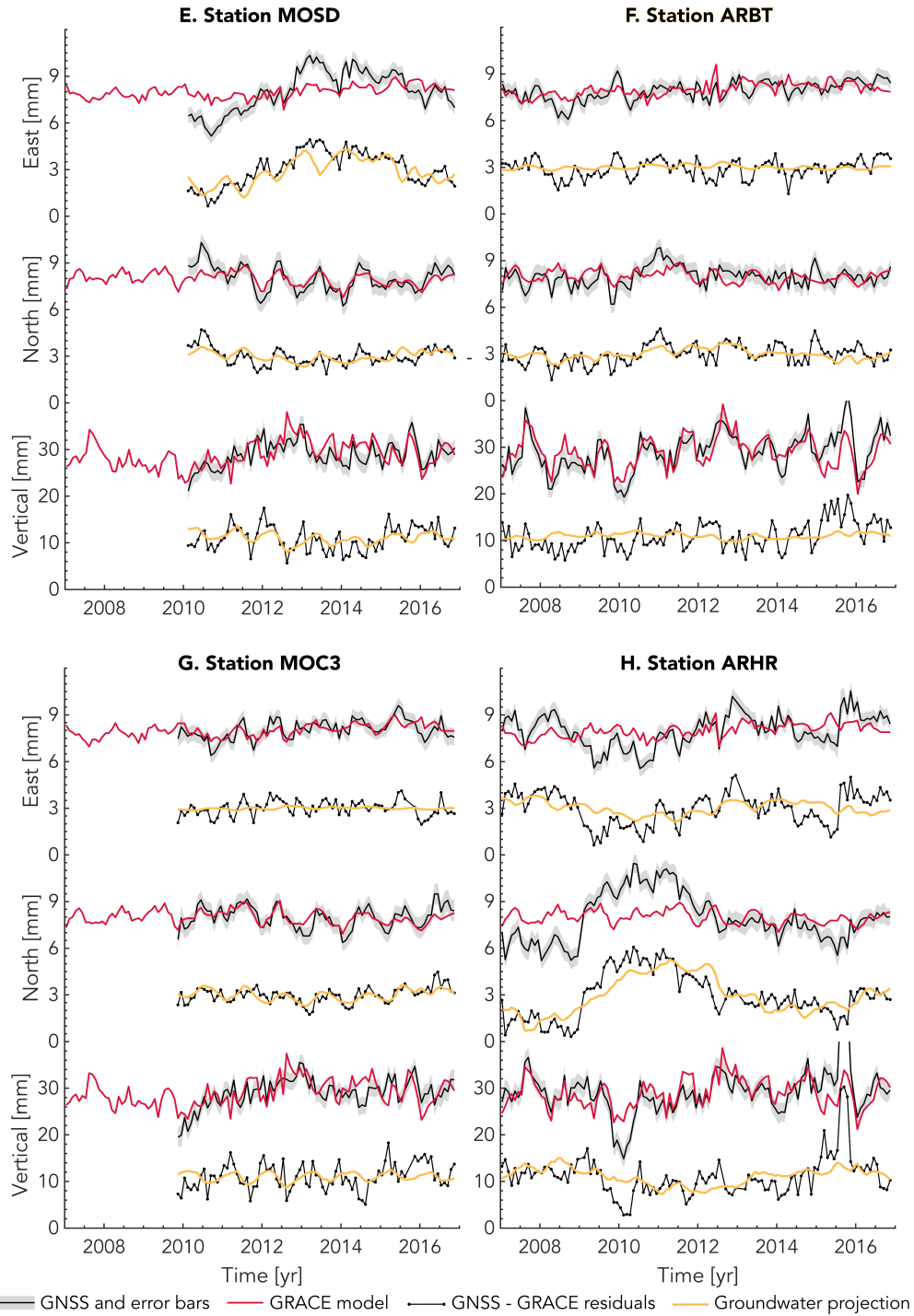


Figure S2: Additional examples of extracted poroelastic signals at different GNSS stations as in Figure 7. Note the different scales for station OKMU.

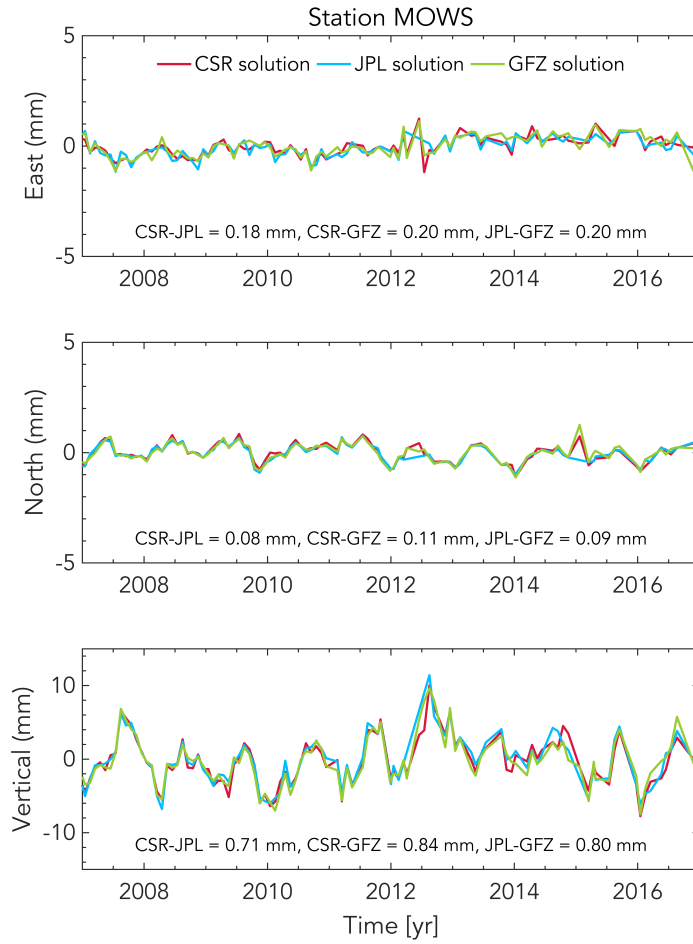


Figure S3: Modeled hydrological elastic loading displacements with different GRACE solutions. The mean absolute deviation between the different solutions are indicated in each subplot.

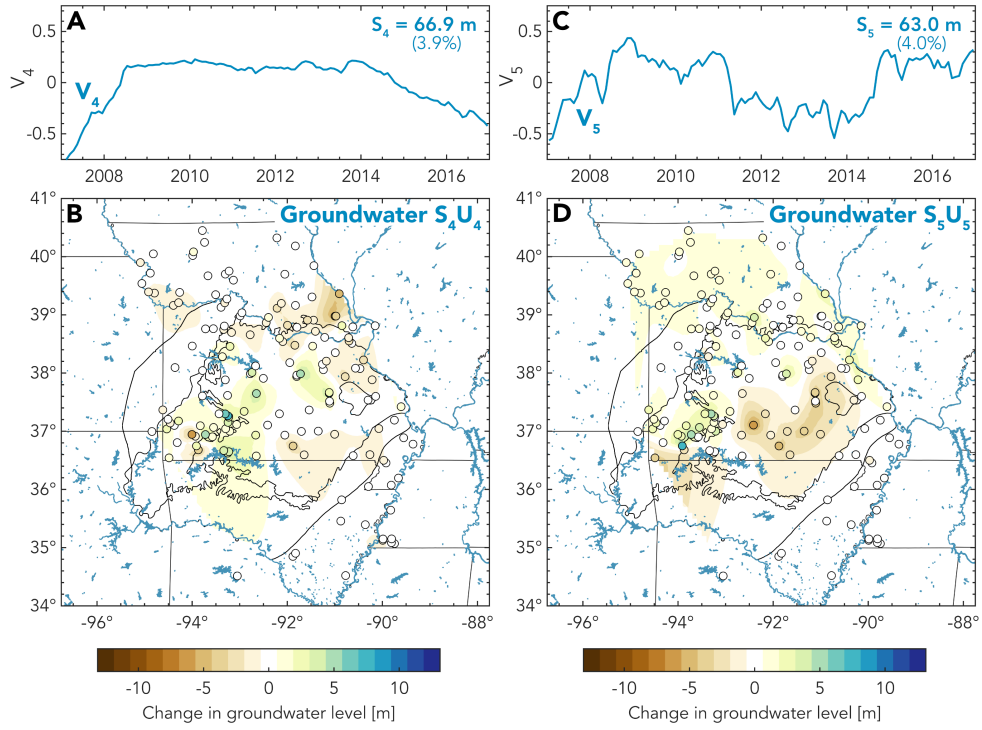


Figure S5: IC4 and IC5 of a 5-components groundwater ICA. IC1, IC2 and IC3 are similar to the 3-components ICA in Figure 5.

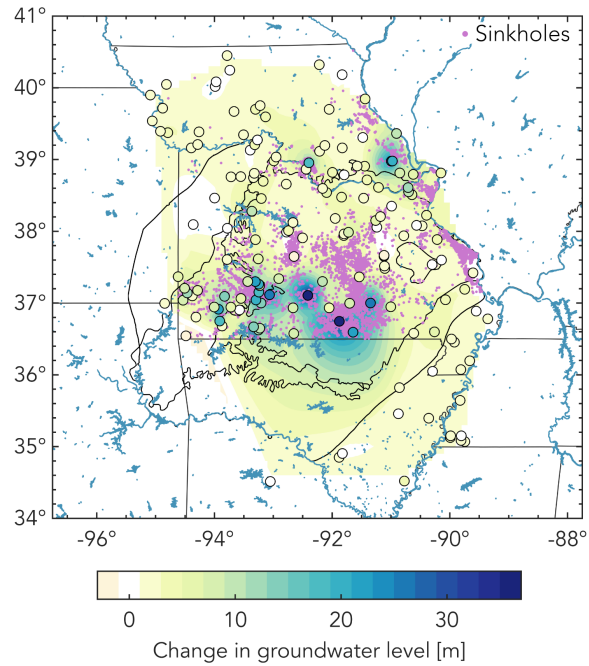


Figure S6: Comparison between the spatial distributions of sinkholes (proxy for karstification) and groundwater IC1. Purple dots indicate the location of known sinkholes in Missouri as reported by the Missouri Geological Survey (<https://dnr.mo.gov/geology/geosrv/envgeo/sinkholes.htm>). The spatial distribution of IC1 groundwater (same as Figure 4B) is shown for comparison.

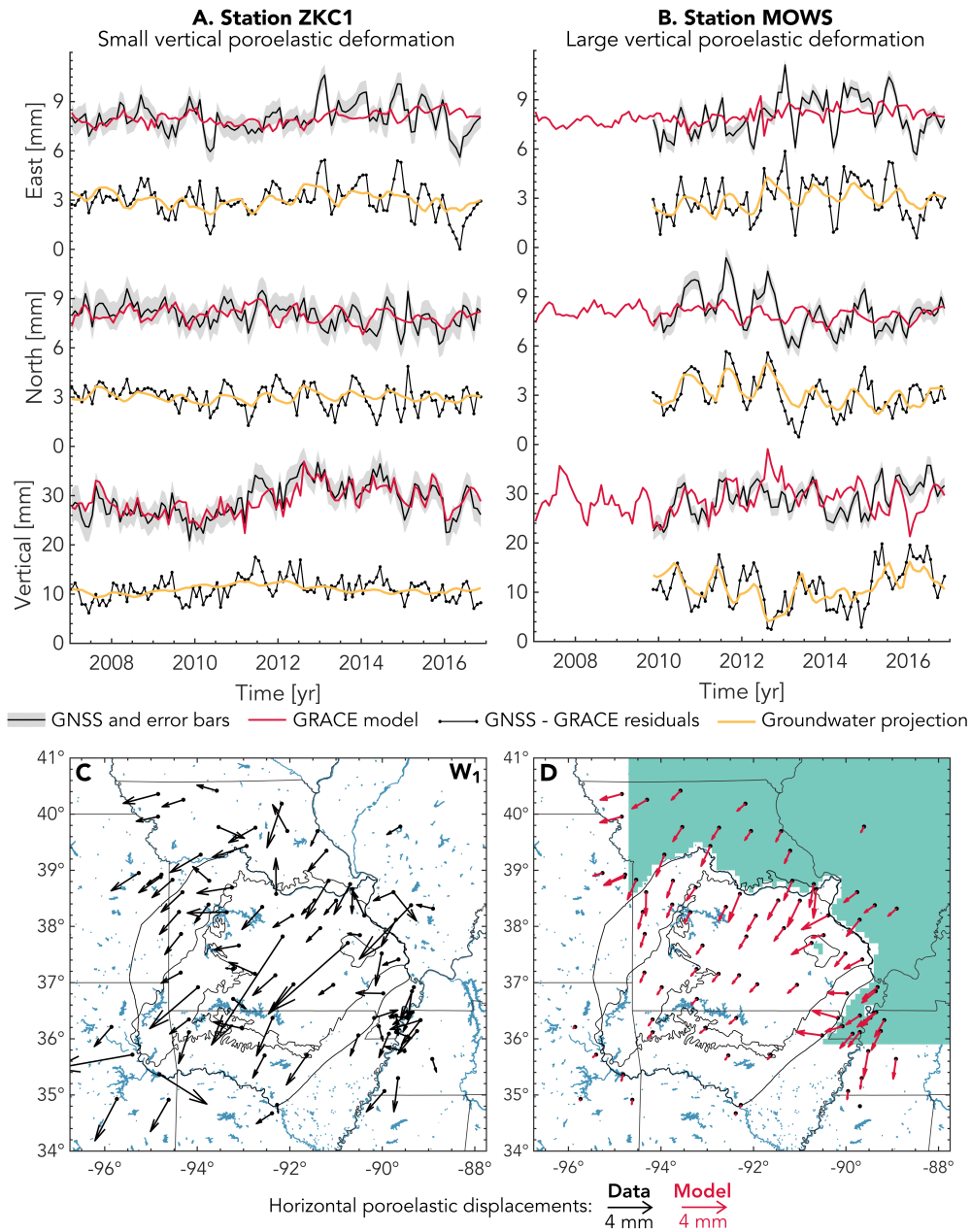


Figure S7: Common mode poroelastic signal from neighbouring aquifers. (A,B) Similar to Figure 7 but without removing horizontal common mode. (C) Horizontal poroelastic displacements inferred by projecting onto W_1 without removing common mode. (D) Modeled horizontal displacements due to poroelastic eigenstrains outside OPAS in turquoise ($\Delta h = 10\text{m}$, $b = 1000\text{m}$).

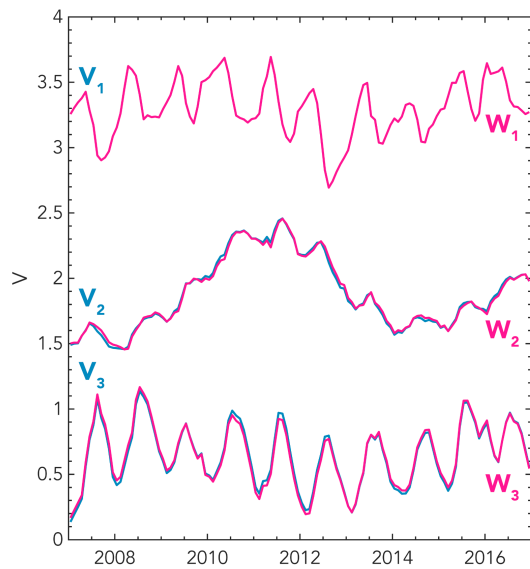


Figure S8: Original groundwater V's vs orthogonalized W's.

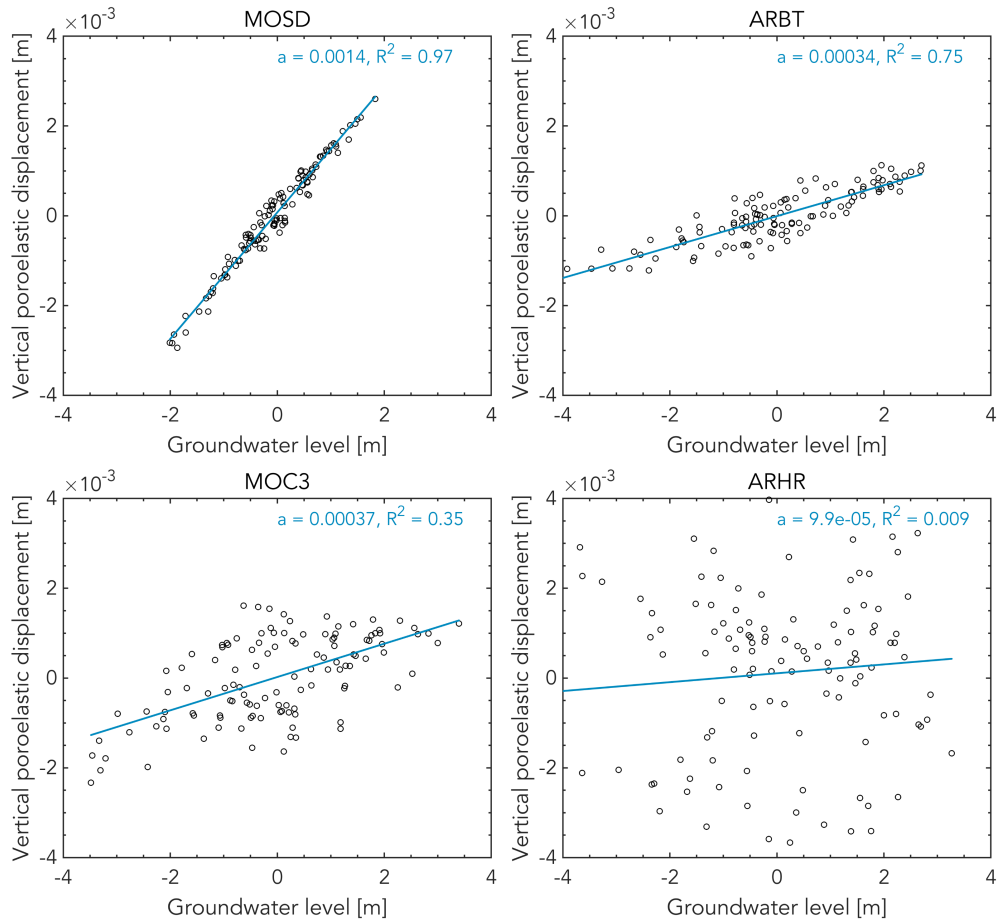


Figure S9: Coefficient of determination for stations shown in Figure 10. a is the slope of the best-fit line.

Rock	Confining stress [MPa]	Poisson ratio	Matrix bulk modulus [MPa]	Young modulus [MPa]
Blair Dolomite	0	0.25	83	125
Maxville Limestone	0	0.23	42	68
Berea Sandstone	10	0.25	6	9
Chattanooga Shale	0	0.16	5	11

Table S1: Elastic properties from Ge & Garven (1992). Note that the Young moduli were computed from the reported values of Poisson ratio and bulk modulus.